Gizatullin, Bulat; Papmahl, Eric; Mattea, Carlos; Stapf, Siegfried:

Quantifying crude oil contamination in sand and soil by EPR spectroscopy

Original published in: Applied magnetic resonance. - Wien [u.a.] : Springer. - 52 (2021), 5, p. 633-648.

Original published: 2021-04-13

ISSN: 1613-7507

DOI: 10.1007/s00723-021-01331-4

[*Visited:* 2021-09-29]

Applied Magnetic Resonance (2021) 52:633–648
https://doi.org/10.1007/s00723-021-01331-4

Applied
Magnetic Resonance

ORIGINAL PAPER

Quantifying Crude Oil Contamination in Sand and Soil by EPR Spectroscopy

Bulat Gizatullin[1] · Eric Papmahl[1] · Carlos Mattea[1] · Siegfried Stapf[1]

Received: 1 February 2021 / Revised: 22 March 2021 / Accepted: 4 April 2021 / Published online: 13 April 2021

Abstract

Crude oil frequently contains stable radicals that allow detection by means of EPR spectroscopy. On the other hand, most sands and soils possess significant amounts of iron, manganese or other metallic species that often provide excessively broad EPR signatures combined with well-defined sharp features by quartz defects. In this study, we demonstrate the feasibility to identify oil contamination in natural environments that are subject to oil spillage during production on land, as well as beachside accumulation of marine oil spillage. Straightforward identification of oil is enabled by the radical contributions of asphaltenes, in particular by vanadyl multiplets that are absent from natural soils. This potentially allows for high-throughput soil analysis or the application of mobile EPR scanners.

1 Introduction

Despite its obvious advantage and high sensitivity in identifying radical species and ion complexes, the documented literature of EPR applications in environmental sciences has been rather limited. Among many reasons are its lack of specificity in the study of metal-containing minerals, and the availability of a wide range of alternative, more established, and possibly more sensitive laboratory methods. However, EPR has developed into an accessible standard method that uses affordable desktop devices which combine satisfactory sensitivity with potential portability. In this respect, EPR is somehow following the development of desktop NMR which dates back decades but has only recently resulted in sophisticated, high-resolution spectrometers which compete with high-field instruments in fields such as education and reaction engineering. Different approaches for truly mobile scanners such as the NMR-MOUSE [1, 2] and other concepts [3–8] have vastly expanded the use of NMR relaxometry and allow its use in field studies, opening up NMR

✉ Siegfried Stapf
Siegfried.stapf@tu-ilmenau.de

[1] FG Technische Physik II/Polymerphysik, Technische Universität Ilmenau, 98684 Ilmenau, Germany

characterization as a method for environmental investigations in situ such as in plants [9, 10] and in soil [11, 12]. However, spectroscopic resolution or the detection of small amounts of contaminants in natural soils is not feasible with single-sided sensors but has to rely on lab-based desktop or high-field instruments. Recently, small and mobile EPR scanners have indeed been suggested that combine portability with the superior detection sensitivity that is known from lab-based EPR instruments as a consequence of the larger electron magnetic moment [13, 14]. See [15] for an overview of recent low-field and portable EPR applications.

Crude oil is a complex mixture of several tens of thousands of known compounds, a fact that needs to be taken into consideration if oil shall be identified by spectroscopic methods. Its ^{1}H NMR signature consists of a broad spectrum representing the unresolved sum of many resonance lines that have tentatively been separated into aromatic and aliphatic regions [16, 17] The distinction of different types of crude oil has been attempted based on quantifying the individual spectral line groups, but the assignment of individual chemicals has not been achieved. It can be assumed that a ^{1}H spectroscopic separation of crude oil in natural soil, against the background of soil organic matter (SOM), is difficult at best [18]. ^{13}C spectroscopy, on the other hand, which is generally used for SOM studies [19, 20], is more challenging for desktop systems, and unfeasible for field work. Much more promising are approaches that include the analysis of relaxation times and diffusion coefficients, as has been successfully demonstrated for oils and brine/oil mixtures in rocks [21, 22]. Oil and water were quantified in oil-containing coastal sands with enhancing the relaxation contrast by addition of manganese salts [23]. While this is an established laboratory method and has been used repeatedly, it is not feasible under in situ conditions where relaxation contrast may be too small. Two-dimensional studies, correlating T_2 relaxation time and diffusion coefficient, succeed in separating oil from water and other fluids [24]. While such experiments can be carried out even on mobile NMR systems such as the NMR-MOUSE, depending on the range of parameters, they can be time-consuming and problematic in terms of quantification.

EPR, on the other hand, is sensitive to detect paramagnetic centers and the unpaired electrons of radicals in the liquid and the solid state, i.e., unlike in NMR the solid component of the sample cannot be neglected. In many types of rocks, the EPR signature is characterized by extremely broad metal ion lines emanating from metallic grains or larger agglomerations, with Fe^{2+} and Fe^{3+} of iron oxides often dominating [25–27]. In addition, individual ions and nanoaggregates generate sharp, well-defined lines as have been observed in metal-containing clays [28, 29]. These consist of singlets and multiplets of Fe or Mn as well as sulfur oxides, for instance [30]. In addition, crystal defects in quartz grains provide narrow and characteristic features close to the Landé factor of the free electron. One particular application of EPR to environmental science aims at the temporal evolution as a consequence of fires [31], while it has been used for decades in archaeological dating [32]; [33] gives an overview of environmental applications of EPR.

While the complexity of features renders a quantitative assessment of the EPR spectrum cumbersome, the large width of the metal grain signal along with the well-defined contributions of manganese, sulfur oxide and other substances makes the

sharp features of isolated ions or radical electrons stand out, in a similar way as the solid contribution to an NMR signal is often negligible or completely suppressed with many detection coils, and only the liquid signal remains.

These particular features provide an opportunity to identify crude oil within a background of natural soil or sand. While by no means all types of oil contain significant amounts of free radicals, most heavy oils have indeed been found to show an EPR signal [34]; see also [35–39] for more recent studies on oil composition. It is commonly assumed that radicals are located in the large polycyclic aromatic hydrocarbons (PAHs), predominantly in asphaltenes, but possibly also in resins [40]. By definition, asphaltenes and resins are characterized by their respective solubility in n-heptane (although other solvents are used in the literature), i.e. asphaltenes precipitate while resins remain in solution, following a classical separation process (SARA [41]), and correlations between the different components and NMR properties have been studied [42]. However, there is no structural difference between both substance classes. In quantitative studies, the EPR signal is found to correlate with the asphaltene content. The NMR relaxation properties of liquid components in oil, the so-called maltenes, were likewise found to correlate with the asphaltene content [43, 44], suggesting that the latter contain the largest amount of unpaired electrons in crude oil, and therefore act as a relaxation agent in analogy to contrast agents in aqueous solution. Current literature concludes that free, delocalized electrons and vanadyl ions (VO^{2+}) constitute the major contributions to the EPR spectrum, though their relative proportion varies greatly. While free electrons lead to a single EPR resonance line, vanadyl ions, which are located in porphyrin rings, give rise to a characteristic octet ($I = 7/2$ for ^{51}V) [45–47]. Only one in ten to a hundred asphaltene molecules contain a radical, therefore they can be considered isolated and are characterized by small linewidths.

The EPR signature of crude oils has been employed for characterization [48], but also for signal enhancement of the remaining maltenes by exploiting the Dynamic Nuclear Polarization (DNP) effect [49]. Related research has been carried out on marine diesel as an important oil byproduct [50, 51].

Considering the rather unspecific proton NMR spectrum, the use of the EPR signal of crude oils appears more promising in their identification as a contaminant to an organic background. In view of the abovementioned specifications, this contribution aims at assessing the conditions necessary for identifying the presence of crude oil in samples of sand and soil, and to give an estimated lower limit for its detection in a routine desktop experiment.

2 Samples and Experiment

In this study, a range of beach sands and soils have been compared in order to cover typical environmental situations; beach sand was used for simulating coastal crude oil spill. FH31, FH32 and W3 sand were obtained from Quarzwerke Frechen, Germany; all other samples were gathered at the given locations (see Table 1). As a representative crude oil sample, Ashalchinskoe heavy oil (Volga-Ural basin, Tatarstan, Russia) has been chosen since its EPR properties are well

Table 1 Abbreviations and origin of sand and soil samples in this study

Sample	Soil/sand	Description	Location	Coordinates
FH31	Sand	Sieved quartz sand	Frechen & Haltern (mixed)	50°55′ N,6°47′ E 51°48′ N,7°15′ E
FH32	Sand	FH31 enriched with Fe_2O_3	dto	dto
W3	Sand	Quartz sand/silt size	Frechen	50°55′ N,6°47′ E
KAL	Soil	Sandy loam	Kaldenkirchen	51°19′ N,6°12′ E
MER	Soil	Silt loam	Merzenhausen	50°56′ N,6°17′ E
SEL	Soil	Silt loam	Selhausen	50°52′ N,6°27′ E
BON	Sand	Beach sand (white)	Bondi Beach, NSW	33°53′ S,151°17′ E
KIN	Sand	Beach sand (white)	Kingscliff, NSW	28°17′ S,153°35′ E
NOU	Sand	Beach sand (white)	Noumea, NC	22°18′ S,166°27′ E
LPS	Sand	Beach sand (black)	La Palma	28°39′ N,17°57′ W
LPV	Mineral	Weathered volcanic rock	La Palma	28°28′ N,17°51′ W
ILM	Soil	Town soil	Ilmenau	50°51′ N,10°55′ E

studied [47, 52]. While being rather viscous, it has an intermediate asphaltene fraction of 4.5% whereas some oil types exceed 15% of asphaltene (see Table 2). From [53] it is known (see Table 3) that the concentration of vanadyl complexes at 7.5×10^{18} spins g^{-1} in asphaltenes is about ten times higher than that of free radicals (8.1×10^{17} spins g^{-1}). In resins, the content of which is about 26% in this oil, the amount is about 9 times lower. In total, radicals contained in Ashalchinskoe oil are contained in the asphaltene and the resin fraction, respectively, in a ratio of about 3:2.

EPR experiments were carried out at a temperature of 300 K on a Miniscope MS-5000 EPR desktop spectrometer (Magnettech, Freiberg Instruments, Germany) operating in X band (9.5 GHz microwave frequency).

Untreated samples (sands, soils as well as crude oil) were first crushed manually with a pestle in order to obtain grain sizes well below the capillaries' inner diameter of 2 mm. All measurements took place inside these 2 mm capillaries, containing about 200 µl of sample volume. Subsequently, 1 g of selected soils were filled into open glass vessels, and the appropriate amount of crude oil added, samples were manually stirred with a spatula for several minutes until a visually homogeneous oil distribution was achieved; 200 µl of these soils were then filled into glass capillaries, before these were flame-sealed.

Depending on the shape of the spectra and the intensity of the spectral lines, experiments were carried out using a number of settings. The modulation frequency was kept constant at 100 kHz and the amplitude was between 0.3 and 0.5 mT unless otherwise noted. Either 0.1 or 1 mW was used as microwave power, and the scanning period was set to 300–500 s for the whole range of magnetic field 50–600 mT.

Prior to concentration dependent measurements, a calibration series was carried out on solutions of TEMPO in n-decane between 0.1 mM and 50 mM which confirmed the linearity of the signal (double integral over the full dispersion spectrum) for all parameter settings used in this study.

Table 2 Physical properties of Ashalchinskoe heavy oil at 20 °C and its composition [53]

Viscosity, mPa s	Density, g cm^{-3}	API gravity	Elemental content, wt.%				SARA analysis, wt. %			
			C	H	N	S	Saturated	Aromatic	Resins	Asphaltenes
2468	0.97	13.8	82.09	10.12	0.63	2.65	26.2 ± 0.5	43.0 ± 0.6	26.3 ± 0.5	4.5 ± 0.3

Table 3 Concentrations of FR and VO^{2+} (from simulation of experimentally obtained spectra in MatLab/Easyspin and comparison with Cu-DETC reference) at $T = 295$ K [53]

	C (VO^{2+}) (spins/g)	C (FR) (spins/g)	C (VO^{2+})/C(FR)
Oil	1.1 (2) 10^{18}	1.2 (1) 10^{17}	9.2
Asphaltene (A)	7.5 (9) 10^{18}	8.1 (9) 10^{17}	9.1
Resin (R)	0.8 (1) 10^{18}	0.9 (1) 10^{17}	9.0

3 Reference EPR spectra

The X-band CW EPR spectrum of Ashalchinskoe crude oil is shown in Fig. 1. Its main features are the free radical (FR) peak at $g = 2.0030$ with a width of approximately 6 G, and the asymmetric octet of the ^{51}V splitting in the VO^{2+} porphyrin molecule. (See [53] and references therein for a detailed discussion of the vanadyl EPR spectrum). These two features are those most frequently encountered in heavy oils, although the relative contribution of VO^{2+} varies significantly. For the purpose of identifying crude oil in an EPR spectrum relative to a background signal, the FR peak and the largest vanadyl peak (representing $m_I = 1/2$) appear to be most suitable.

Figure 2 presents an overview of EPR spectra of all types of soil and sand employed in this study; all measurements were carried out with a microwave power of 0.1 mW and a modulation amplitude of 0.3 mT. Note the different amplitude scales, while all samples contained identical sample volumes. The predominant property of these spectra is an extremely broad background signature arising from Fe ions in unspecified environment. The two by far largest signals

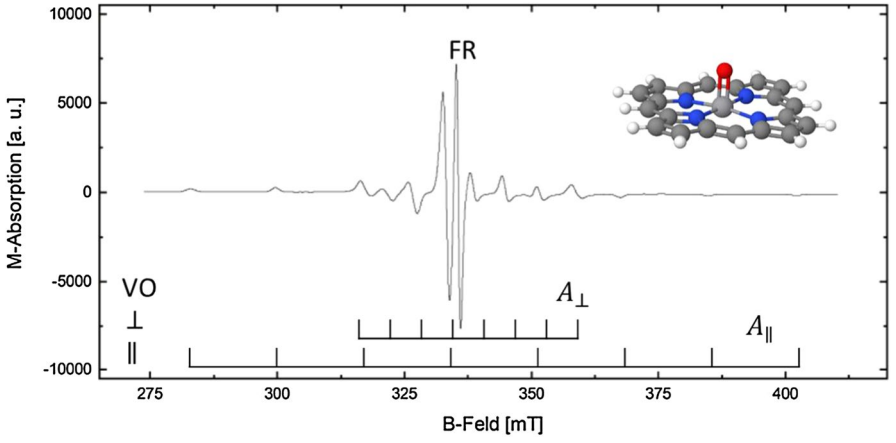

Fig. 1 EPR spectrum of Ashalchinskoe crude oil, with coupling constants for the VO^{2+} multiplet indicated. FR refers to Free Radicals. The inset shows the vanadyl porphyrin which is expected to occur as part of the PAH of asphaltene molecules [53]

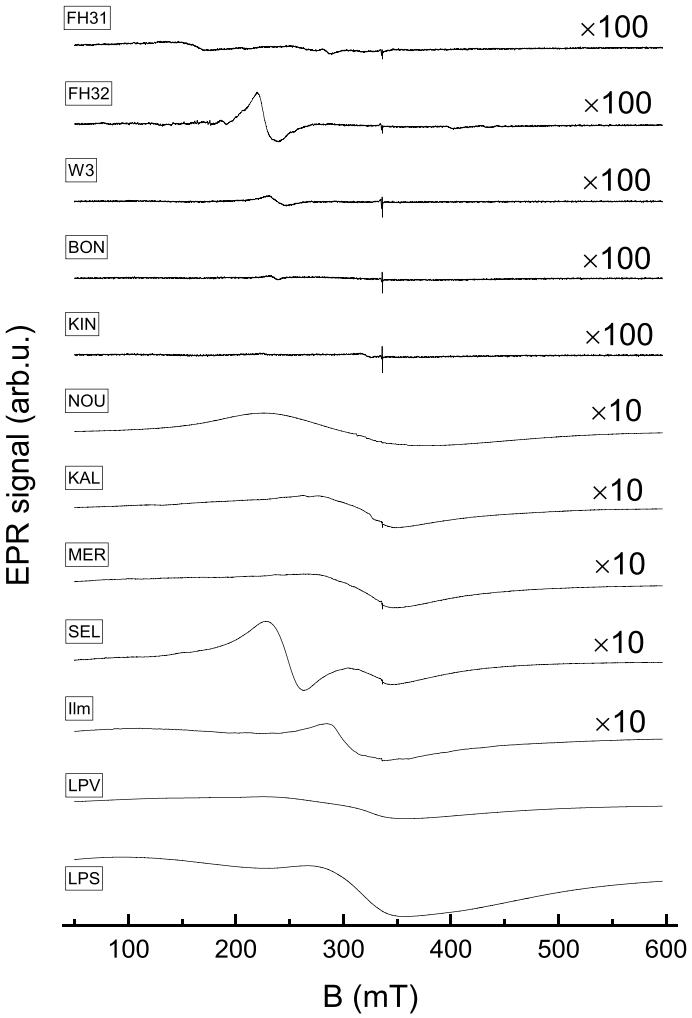

Fig. 2 EPR CW spectra of all dry sand and soil samples studied in this work. Note that three different scales have been used in order to accommodate the whole range of signal intensities

(two bottom spectra) correspond to volcanic rocks and sand from La Palma island, which can tentatively be decomposed into two separate contributions.

While it is beyond the purpose of this study, a rough estimation of the Fe content can be obtained by comparison with soil samples with known metal content; the result is about 26% for LPS and 11% for LPV. These figures are probably overestimated due to the excessive width of the EPR signal, but are in qualitative agreement with values indicated for La Palma basaltic sand of between 17 and 21% FeO [54]. These are among the highest Fe contents occurring naturally on Earth, and we have refrained from carrying out oil contamination experiments on these samples, although they might indeed be feasible in the center part of the EPR spectrum.

Excluding the La Palma basalt samples, the remaining spectra can be separated into two groups, five sands and four soils. Again, the predominant contribution is iron, mostly in the form of FeO and Fe_2O_3 as well as of Fe hydroxides such as Goethite. Within typical errors of about ±10%, the ratios of the double integral over the broad line are proportional to elementary Fe weight content obtained from ICP-OES (Inductively Coupled Plasma Optical Emission Spectroscopy), i.e. 1.89 wt-% for MER, 2.08 wt-% for SEL and 0.71% for KAL (see Table 4). The influence of these Fe ions on the NMR relaxation of water protons has been studied earlier [55]. Also obtained by this method were concentrations of 0.014 wt-% for FH31 and 0.15 wt-% for FH32, sand artificially enriched with iron oxide. Employing these data, we could fit approximate iron concentrations for the remaining samples, and obtained 1.81 wt-% for ILM, 1.4 wt-% for NOU, 0.02 wt-% for W3, and about 0.002–0.003 wt-% for BON and KIN.

The four soil samples apparently represent typical spectra for iron contents in the range of a few percent, whereas clean quartz sand can possess up to three orders of magnitude less iron. The pronounced peak in FH32 about $g = 2.98$ is a consequence of the addition of iron predominantly in the form of Fe hydroxide. Among the sands, NOU is somewhat different since it represents a metal-rich source (see below).

An additional contribution, however, will become important if small amounts of oil must be detected. The sharp feature visible in Fig. 2, and magnified in Fig. 3/top for several of the sand samples, represents naturally occurring crystal defects in quartz. It appears at 336,1 mT, corresponding to $g = 2.01$, and is attributed to the well-known E' defects of oxygen vacancies in quartz [56, 57]. Its width is between 2.5 and 3 G. Nouméa sand (taken at a beach close to the city, Fig. 3/center) differs not only by its larger iron content but also by the fact that a small quartz defect peak at 335.6 mT ($g = 2.02$) is superposed onto a Mn^{2+} sextet, in agreement with a Mn concentration of 0.2% or larger (see magnification in Fig. 3/bottom). It is well-known that New Caledonian minerals, apart from possessing one of the world's largest nickel reservoir, do also contain high concentrations of MgO of up to 21%.

Table 4 Metal content of selected soils and sand, obtained from ICP-OES (c/o Andreas Pohlmeier, FZ Jülich)

Sample	Fe wt [%] SD [%]	Mn wt [%] SD [%]	Cu wt [%] SD [%]	Ca wt [%] SD [%]	Mg wt [%] SD [%]
MER	1.89 0.03	0.071 0.002	0.0044 0.0003	0.537 0.007	0.326 0.004
SEL	2.083 0.017	0.0827 0.0009	< 0.002	0.509 0.003	0.357 0.006
KAL	0.712 0.014	0.037 0.002	< 0.002	0.161 0.002	0.074 0.003
FH31	0.0138 0.0015	< 0.0005	< 0.002	0.0074 0.0006	< 0.00008
FH32	0.149 0.007	< 0.0005	< 0.002	0.0101 0.0006	< 0.00008

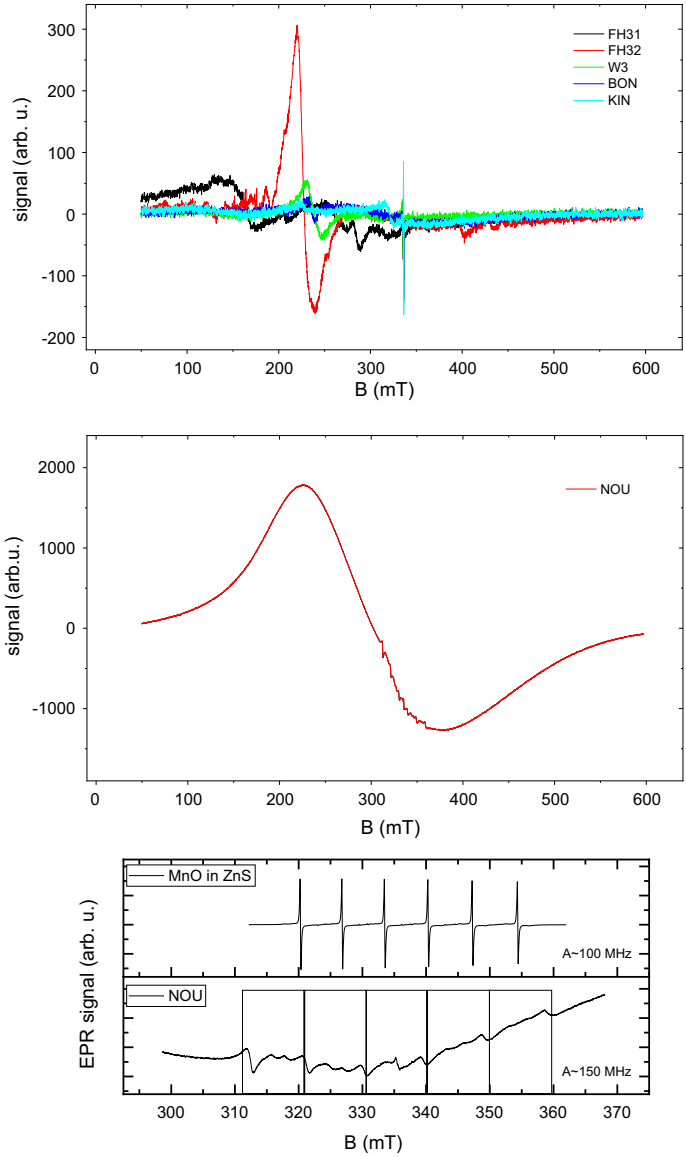

Fig. 3 (Top) EPR CW spectra for several dry sands; all spectra are plotted on the same scale and were acquired with the same parameters; (center) EPR CW spectrum for Nouméa (NOU) sand; (bottom) magnification of the central part of the NOU spectrum after baseline correction with equal line distances indicated by rectangles—a spectrum of MnO in ZnS is shown for comparison as an example of a highly symmetrical Mn sextet spectrum

4 Results for Oil Contaminated Soils

In order to test the feasibility of detecting oil contamination in soil, two sand samples (FH32 and Bondi Beach) and one soil (Kaldenkirchen) were prepared with concentrations in the range from 0.5 to 9 wt-% of Ashalchinskoe oil.

The iron peak in FH32 is centered about $g = 2.98$ and is outside the center region of the spectrum; the spectrum upward from 300 mT is therefore comparable to a native sand without added Fe.

Figure 4 demonstrates the prominence of the crude oil EPR signal in the FH32 sand sample. In this representation, the free radical peak of oil and the quartz defect peak, both in the region between 335 and 336 mT, overlap; the largest VO^{2+} peak at 333.4 mT becomes distinct. The presence of oil, however, is clearly visible. An initial attempt to determine the oil content from a double integral of the full range of Fig. 4, and taking the expected number of spins in the crude oil sample into account, delivers an amount of 0.6%. By proper fitting of the actual crude oil spectral features, if these were available for the sample under study such as in the case of a known spillage situation, this quantitation can possibly be improved significantly.

Figure 5 compares the spectra obtained with oil in Bondi Beach sand at different weight fractions. The double integral over this frequency range provides a rather good correlation with oil content (Pearson's coefficient 0.9988), even though absolute values are hard to obtain—this would require a separate calibration. (Integration over a narrower range 336… 337 mT gives a slightly lower correlation coefficient). Nevertheless, oil fractions from 0.5% can be detected with certainty, and become quantitative at least from 1% upward.

For the situation with KAL, a typical soil, the background signal emanating from Fe ions is much more dominant, and needs to be subtracted assuming a polynomial

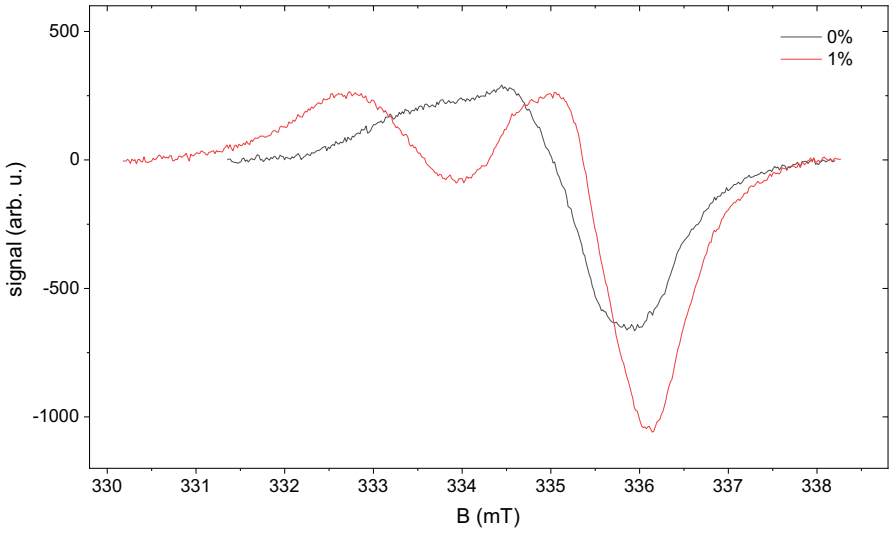

Fig. 4 EPR CW spectra for FH32 sand with and without 1 wt% Ashalchinskoe crude oil

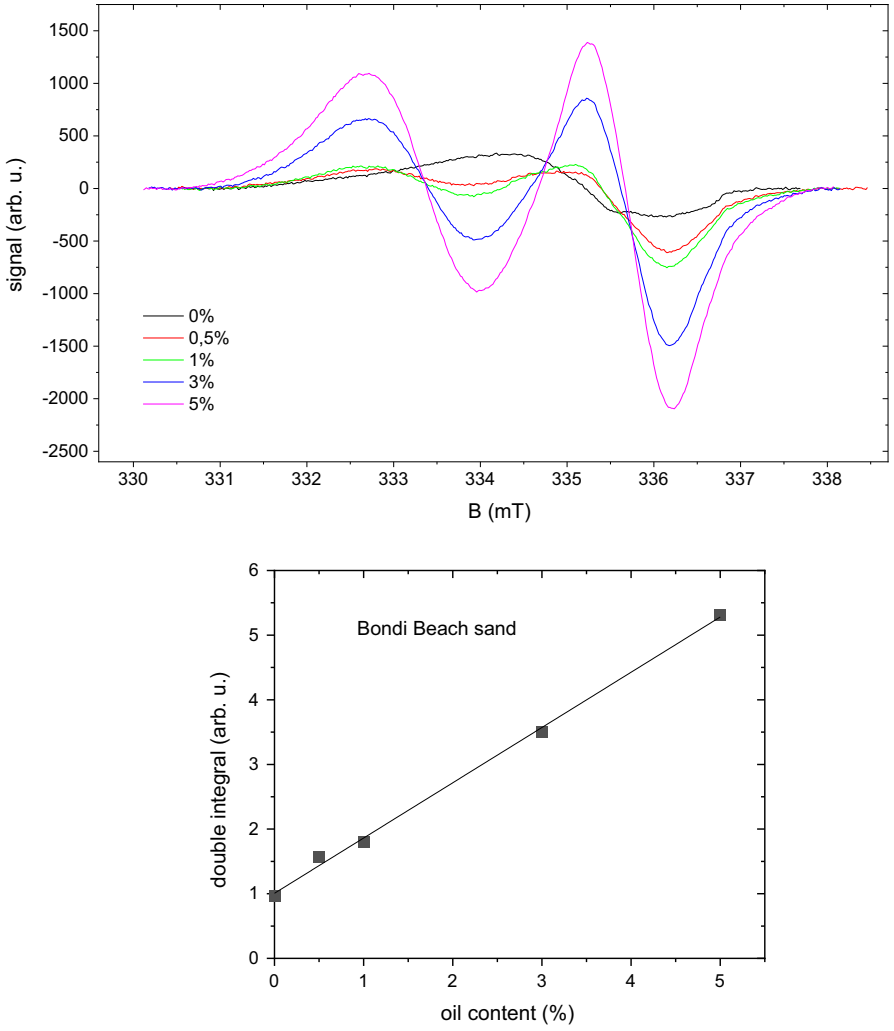

Fig. 5 top: EPR CW spectra for Bondi Beach sand (BON) with different concentrations of Ashalchinskoe crude oil—only the center region of the spectrum is shown after baseline subtraction; bottom: Double integral for the EPR signal obtained from the spectrum (whole range), including linear regression fit

function that provides minimum background in the central region of the spectrum. The total integral correlates with the oil concentration but the minimum concentration that can be safely detected is on the order of 3%; a better correlation is obtained when the integral is carried out over the single line between about 336 and 337 mT, than by integration over the wider range 329–339 mT (Pearson's correlation coefficient of 0.967 as compared to 0.939). Figure 6 shows the spectra before and after background correction as well as the double integral of the narrow integration region. In all attempts to establish a correlation between signal intensity and weight of oil it must be considered that the actual amount of radical-containing oil

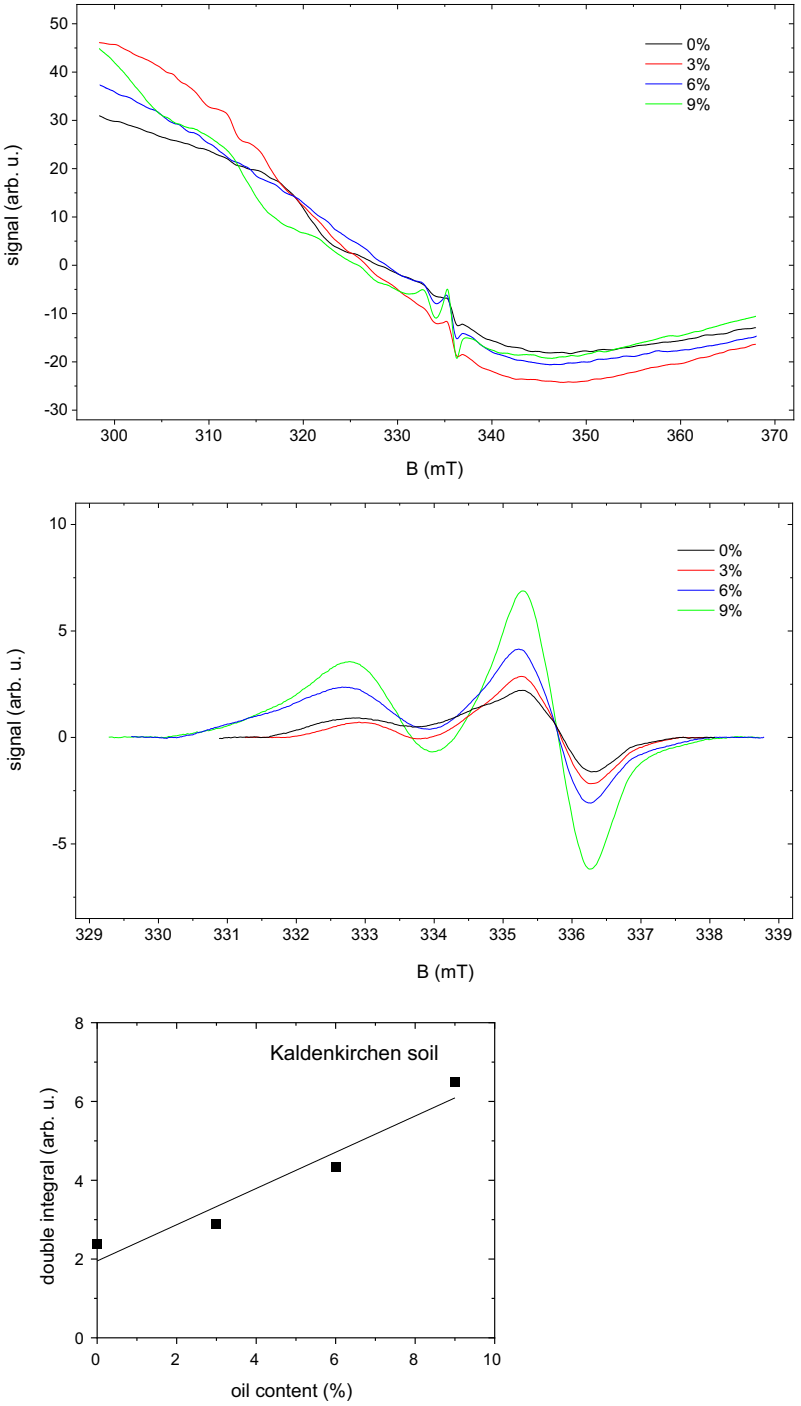

Fig. 6 EPR CW spectra for Kaldenkirchen soil (KAL) with different concentrations of crude oil, (top) before and (center) after background subtraction; (bottom) double integral for the range 336 … 337 mT

components within the 200 µl sample volume may differ from the average determined within the larger volume of the prepared soil/oil mixture due to heterogeneities in the distribution; this also affects the overall metal content in the measured sample and its influence onto the background signal. Wherever possible, larger sample volumes or repetitive measurements of different samples will increase the precision in quantitation in a dedicated laboratory study or in portable scanner applications.

5 Conclusions

EPR single-scan spectra on a desktop spectrometer operating at X band demonstrate that detection of the presence of a typical crude oil is feasible due to a combination of either its vanadyl ion or its free radical signature. While the free radical is found more commonly in oil, it tends to overlap with a sharp line emanating from crystal defects in quartz structures. However, even with a spectrometer possessing low resolution such as might be expected from a portable solution, oil can be identified by integrating over the region about this central peak and comparing it to the signal from an uncontaminated sample. The VO^{2+} central peak of $m_I=+1/2$, wherever present, is more distinct and can be employed for a better quantitation of the oil content. In clean sands, such as would be encountered in shoreline oil spillage, a detection limit of well below 1% of oil was obtained for laboratory conditions, and 0.1% appears entirely feasible; reliable quantitation is possible at least from 1% upward, and more detailed modelling with the lineshape of the bulk crude oil will reduce this limit significantly. For typical soils of 1–2 wt-% iron content, oil detection is still possible down to about 1% due to the narrow lines in comparison to the very broad spectral background of the iron containing compounds, but quantitation requires more elaborate treatment of the background signal. One possibility could be the use of an internal standard with a defined line intensity, preferably not overlapping with the spectral features expected from oil.

As a method for high-throughput serial sampling, where precise oil concentrations are of less immediate interest, EPR of soil/crude mixtures can serve as a routine scanning method for oil fractions of 1% or less. This amount is difficult to study even by conventional low-field NMR spectroscopy, particularly in the presence of soil organic matter, and is below the resolution limit of most relaxation/diffusion NMR studies reported so far. EPR thus does have an advantage over many NMR methods. With the properties of oil EPR spectra known from the literature, a dedicated narrow-range EPR scan will further reduce the total experimental time for a single scan, and can therefore bring mobile EPR equipment, typically operating at low microwave frequencies, into the range of operative sensors for identifying oil spillage in sand and soil environments.

Acknowledgements We gratefully acknowledge A. Pohlmeier for providing soil samples and analyses and for help in the interpretation of EPR spectra; fruitful discussion with M. Gafurov in the context of oil EPR signal interpretation is gratefully acknowledged.

Funding Open Access funding enabled and organized by Projekt DEAL.

References

1. G. Eidmann, R. Savelsberg, P. Blümler, B. Blümich, The NMR MOUSE, a mobile universal surface explorer. J. Magn. Reson. A **122**, 104–109 (1996)
2. B. Blümich, S. Haber-Pohlmeier, W. Zia (eds.), *Compact NMR* (de Gruyter, Berlin/Boston, 2014)
3. P.J. McDonald, P.S. Aptaker, J. Mitchell, M. Mulheron, A unilateral NMR magnet for sub-structure analysis in the built environment: the Surface GARField. J. Magn. Reson. **185**, 1–11 (2007)
4. B. Manz, A. Coy, R. Dykstra, C.D. Eccles, M.W. Hunter, B.J. Parkinson, P.T. Callaghan, A mobile one-sided NMR sensor with a homogeneous magnetic field: the NMR-MOLE. J. Magn. Reson. **183**, 25–31 (2006)
5. W.H. Chang, J.H. Chen, L.P. Hwang, Single-sided mobile NMR with a Halbach magnet. Magn. Reson. Imaging **24**, 1095–1102 (2006)
6. S. Utsuzawa, E. Fukushima, Unilateral NMR with a barrel magnet. J. Magn. Reson. **282**, 104–113 (2017)
7. S. Oligschläger, S. Glöggler, J. Watzlaw, K. Brendel, D. Jaschtschuk, J. Colell, W. Zia, M. Vossel, U. Schnakenberg, B. Blümich, A miniaturized NMR-MOUSE with a high magnetic field gradient (Mini-MOUSE). Appl. Magn. Reson. **46**, 181–202 (2015)
8. M. Greer, C. Chen, S. Mandal, An easily reproducible, hand-held, single-sided, MRI sensor. J. Magn. Reson. **308**, 106591 (2019)
9. D. Capitani, F. Brilli, L. Mannina, N. Proietti, F. Loreto, In situ investigation of leaf water status by portable unilateral nuclear magnetic resonance. Plant Physiol. **149**, 1638–1647 (2009)
10. A. Nagata, K. Kose, Y. Terada, Development of an outdoor MRI system for measuring flow in a living tree. J. Magn. Reson **265**, 129–138 (2016)
11. O. Sucre, A. Pohlmeier, A. Miniere, B. Blümich, Low-field NMR logging sensor for measuring hydraulic parameters of model soils. J. Hydrology **406**, 30–38 (2011)
12. S. Merz, A. Pohlmeier, J. Vanderborght, D. van Dusschoten, H. Vereecken, Transition of stage I to stage II evaporation regime in the topmost soil: high-resolution NMR imaging, profiling and numerical simulation. Microporous Mesoporous Mat. **205**, 3–6 (2015)
13. L.E. Switala, W.J. Ryan, M. Hoffman, W. Brown, J.P. Hornak, Low frequency EPR and EMR point spectroscopy and imaging of a surface. Magn Reson Imaging **34**, 469–472 (2016)
14. L.E. Switala, B.E. Black, C.A. Mercovich, A. Seshadri, J.P. Hornak, An electron paramagnetic resonance mobile universal surface explorer. J Magn Reson **285**, 18–25 (2017)
15. J.R. Biller, J.E. McPeak, EPR Everywhere. Appl Magn Reson (2021). https://doi.org/10.1007/s00723-020-01304-z
16. A. Adhvaryu, J.M. Perez, L.J. Duda, Quantitative NMR spectroscopy for the prediction of base oil properties. Tribol. Trans. **43**, 245–250 (2000)
17. S. Ok, T. Mal, NMR spectroscopy analysis of asphaltenes. Energy Fuels **33**, 10391–10414 (2019)
18. C.M. Preston, Applications of NMR to soil organic matter analysis: history and prospects. Soil Sci. **161**, 144–166 (1999)
19. N. Mahieu, E.H. Randall, D.S. Powlson, Statistical analysis of published carbon-13 CPMAS NMR spectra of soil organic matter. Soil Sci. Soc. Am. J. **63**, 307–319 (1999)
20. I. Kögel-Knabler, Analytical approaches for characterizing soil organic matter. Org. Geochem. **31**, 609–625 (2000)

21. M.D. Hürlimann, L. Venkataramanan, C. Flaum, The diffusion-spin relaxation time distribution function as an experimental probe to characterize fluid mixtures in porous media. J. Chem. Phys. **117**, 10223–10232 (2002)
22. J. Mitchell, T.C. Chandrasekera, D.J. Holland, L.F. Gladden, E.J. Fordham, Magnetic resonance imaging in laboratory petrophysical core analysis. Phys. Rep. **526**, 165–225 (2013)
23. N. Bai, D. Wang, Y. Zhang, H. Sui, Determination of water and oil in contaminated coastal sand by low-field hydrogen-1 nuclear magnetic resonance (1H NMR). Anal Lett (2020). https://doi.org/10.1080/00032719.2020.1808009
24. E.L. Fay, R.J. Knight, Detecting and quantifying organic contaminants in sediments with nuclear magnetic resonance. Geophysics **81**, EN87-97 (2016)
25. G.P. Kayukova, A.N. Mikhailova, N.M. Khasanova, V.P. Morozov, A.V. Vakhin, N.A. Nazimov, O.S. Sotnikov, R.S. Khisamov, Influence of hydrothermal and pyrolysis processes on the transformation of organic matter of dense low-permeability rocks from domanic formations of the romashkino oil field. Geofluids **2018**, 1–14 (2018)
26. A. Bhattacharyya, M.P. Schmidt, E. Stavitski, C.E. Martínez, Iron speciation in peats: chemical and spectroscopic evidence for the co-occurrence of ferric and ferrous iron in organic complexes and mineral precipitates. Org. Geochem. **115**, 124–137 (2018)
27. A. Pwa, J.C. van Moort, Electron paramagnetic resonance (EPR) spectroscopy in massive sulphide exploration, Rosebery mine area, western Tasmania, Australia. J Geochem Exploration **65**, 155–172 (1999)
28. T.J. Punnavaia, Chapter 6 electron spin resonance studies of clay minerals, developments in sedimentology, 34, 139–161 in: Advanced techniques for clay mineral Analysis, J.J. Fripiat (Ed.), Elsevier 1982
29. P. Hall, The application of electron spin resonance spectroscopy to studies of clay minerals: II. Interlamellar complexes—structure, dynamics and reactions. Clay Miner. **15**, 337–349 (1980)
30. N.M. Khasanova, D.T. Gabdrakhmanov, G.P. Kayukova, A.N. Mikhaylova, V.P. Morozov, EPR study of hydrocarbon generation potential of organic-rich domanik rocks. Magn. Reson. Solids **19**, 17102 (2017)
31. M. Jerzykiewicz, G. Barančíková, E. Jamroz, A. Kałuża-Haładyn, Application of EPR spectroscopy in studies of soils from destroyed forests. Appl. Magn. Reson. **50**, 753–760 (2019)
32. W.J. Rink, Electron spin resonance (ESR) dating and ESR applications in quaternary science and archaeometry. Radiat. Meas. **27**, 975–1025 (1997)
33. C.J. Rhodes, Applications of EPR in the Environmental Sciences, in: EPR of Free Radicals in Solids II, A. Lund, M. Shiotani (eds.), Springer Netherlands, (2012)
34. H.S. Gutowsky, B.R. Ray, R.L. Rutledge, R.R. Unterberger, Carbonaceous free radicals in crude petroleum. J. Chem. Phys. **28**, 744–745 (1958)
35. K. Ben Tayeb, O. Delpoux, J. Barbier, J. Marques, J. Verstraete, H. Vezin, Applications of pulsed electron paramagnetic resonance spectroscopy to the identification of vanadyl complexes in asphaltene molecules. Part 1: influence of the origin of the feed. Energy Fuels **29**, 4608–4615 (2015)
36. K. Ben Tayeb, O. Delpoux, J. Barbier, P. Chatron-Michaud, M. Digne, H. Vezin, Applications of pulsed electron paramagnetic resonance spectroscopy to the identification of vanadyl complexes in asphaltene molecules. Part 2: hydrotreatment monitoring. Energy Fuels **31**, 3288–3294 (2017)
37. M.S. Hernández, D.S. Coll, P.J. Silva, Temperature dependence of the electron paramagnetic resonance spectrum of asphaltenes from venezuelan crude oils and their vacuum residues. Energy Fuels **33**, 990–997 (2019)
38. M.S. Hernández, P.J. Silva, Electron paramagnetic resonance study of the fractions and trapped compounds in asphaltenes of merey heavy crude oils and its vacuum residue. Energy Fuels **34**, 5641–5651 (2020)
39. G.V. Mamin, M.R. Gafurov, R.V. Yusupov, I.N. Gracheva, Yu.M. Ganeeva, T.N. Yusupova, S.B. Orlinskii, Toward the asphaltene structure by electron paramagnetic resonance relaxation studies at high field (3.4T). Energy Fuels **30**, 6942–6946 (2016)
40. N.A. Mironov, G.R. Abilova, Y.Y. Borisova, E.G. Tazeeva, D.V. Milordov, S.G. Yakubova, M.R. Yakubov, Comparative study of resins and asphaltenes of heavy oils as sources for obtaining pure vanadyl porphyrins by the sulfocationite-based chromatographic method. Energy Fuels **32**, 12435–12446 (2018)
41. N. Aske, H. Kallevik, J. Sjoblom, Determination of saturate, aromatic, resin, and asphaltenic (SARA) components in crude oils by means of infrared and near-infrared spectroscopy. Energy Fuels **15**, 1304–1312 (2002)

42. F. Sanchez-Minero, J. Ancheyta, G. Silva-Oliver, S. Flores-Valle, Predicting SARA composition of crude oil by means of NMR. Fuel **110**, 318–321 (2013)
43. S. Stapf, A. Ordikhani-Seyedlar, N. Ryan, C. Mattea, R. Kausik, D.E. Freed, Y.-Q. Song, M.D. Hürlimann, Probing maltene-asphaltene interaction in crude oil by means of NMR relaxation. Energy Fuels **28**, 2395–2401 (2014)
44. J.J. Chen, M. Hürlimann, J. Paulsen, D. Freed, S. Mandal, Y.-Q. Song, Dispersion of T1 and T2 nuclear magnetic resonance relaxation in crude oils. ChemPhysChem **15**, 2676–2681 (2014)
45. H.-L. Chang, G.K. Wong, J.R. Lin, T. Yen, *Asphaltenes and Asphalts. 2. Developments in Petroleum Science* (Elsevier, Amsterdam, 2000), pp. 229–280
46. D. Gourier, O. Delpoux, A. Bonduelle, L. Binet, I. Ciofini, H. Vezin, EPR, ENDOR, and HYSCORE study of the structure and the stability of vanadyl-porphyrin complexes encapsulated in silica: potential paramagnetic biomarkers for the origin of life. J Phys Chem B **114**, 3714–3725 (2010)
47. T.B. Biktagirov, M.R. Gafurov, M.A. Volodin, G.V. Mamin, A.A. Rodionov, V.V. Izotov, A.V. Vakhin, D.R. Isakov, S.B. Orlinskii, Electron paramagnetic resonance study of rotational mobility of vanadyl porphyrin complexes in crude oil asphaltenes: probing the effect of thermal treatment of heavy oils. Energy Fuels **28**, 6683–6687 (2014)
48. L.W. Kiruri, B. Dellinger, S. Lomnicki, Tar balls from deep water horizon oil spill: environmentally persistent free radicals (EPFR) formation during crude weathering. Environ. Sci. Technol. **47**, 4220–4226 (2013)
49. E. Poindexter, An overhauser effect in natural crude oil. Nature **182**, 1087 (1958)
50. M.T. Piccinato, C.L.B. Guedes, E. Di Mauro, EPR characterization of organic free radicals in marine diesel. Appl. Magn. Reson. **35**, 379–388 (2009)
51. A.C. Gomes Mantovani, L.T. Chendynski, A. Salviato, D. Borsato, V.T. Santana, E. Di Mauro, Monitoring free radicals formation in the biodiesel oxidation reaction via electronic paramagnetic resonance. Fuel **224**, 255–260 (2018)
52. M.R. Gafurov, M.A. Volodin, A.A. Rodionov, A.T. Sorokina, M.Y. Dolomatov, A.V. Petrov, A.V. Vakhin, G.V. Mamin, S.B. Orlinskii, EPR study of spectra transformations of the intrinsic vanadyl-porphyrin complexes in heavy crude oils with temperature to probe the asphaltenes' aggregation. J. Petrol. Sci. Eng. **166**, 363–368 (2018)
53. B. Gizatullin, M. Gafurov, A. Vakhin, A. Rodionov, G. Mamin, S. Orlinskii, C. Mattea, S. Stapf, Native vanadyl complexes in crude oil as polarizing agents for in situ proton dynamic nuclear polarization. Energy Fuels **33**, 10923–10932 (2019)
54. S. Weyer, H.-M. Seitz, Coupled lithium- and iron isotope fractionation during magmatic differentiation. Chem. Geology **294**, 42–50 (2012)
55. S. Haber-Pohlmeier, S. Stapf, A. Pohlmeier, NMR fast field cycling relaxometry of unsaturated soils. Appl. Magn. Reson. **45**, 1099–1115 (2014)
56. F.J. Feigl, J.H. Anderson, Defects in crystalline quartz—electron paramagnetic resonance of E' vacancy centers associated with germanium impurities. J. Phys. Chem. Solids **31**, 575–596 (1970)
57. R.A. Weeks, Paramagnetic resonance of lattice defects in irradiated quartz. J. Appl. Phys. **27**, 1376–1381 (1956)